The Journal of Chemical Physics

RESEARCH ARTICLE | MARCH 25 2024

Deciphering the irradiation induced fragmentation–rearrangement mechanisms in valence ionized CF_3CH_2F

Special Collection: 2024 JCP Emerging Investigators Special Collection

Víctor S. A. Bonfim ; Cauê P. Souza ; Daniel A. B. de Oliveira ; Leonardo Baptista ; Antônio C. F. Santos ; Felipe Fantuzzi

J. Chem. Phys. 160, 124308 (2024)
https://doi.org/10.1063/5.0188201

AIP Publishing

The Journal of Chemical Physics ARTICLE pubs.aip.org/aip/jcp

Deciphering the irradiation induced fragmentation–rearrangement mechanisms in valence ionized CF_3CH_2F

Cite as: J. Chem. Phys. 160, 124308 (2024); doi: 10.1063/5.0188201
Submitted: 20 November 2023 • Accepted: 27 February 2024 •
Published Online: 25 March 2024

Víctor S. A. Bonfim,[1,2,a)] Cauê P. Souza,[1] Daniel A. B. de Oliveira,[3] Leonardo Baptista,[4] Antônio C. F. Santos,[2,b)] and Felipe Fantuzzi[1,c)]

AFFILIATIONS

[1] School of Chemistry and Forensic Science, University of Kent, Canterbury CT2 7NH, United Kingdom
[2] Instituto de Física, Universidade Federal do Rio de Janeiro, Av. Athos da Silveira Ramos 149, 21941-909 Rio de Janeiro, Brazil
[3] Universidade Federal do Norte do Tocantins, Lot. Araguaína Sul, 77826-612 Araguaína, Brazil
[4] Departamento de Química e Ambiental, Universidade do Estado do Rio de Janeiro, Rodovia Presidente Dutra km 298, 27537-000 Rio de Janeiro, Brazil

Note: This paper is part of the 2024 JCP Emerging Investigators Special Collection.
[a)] **Current address:** Centro Internacional de Física, Instituto de Física, Universidade de Brasilia, 70910-900 Brasilia, Brazil.
[b)] toni@if.ufrj.br
[c)] **Author to whom correspondence should be addressed:** f.fantuzzi@kent.ac.uk

ABSTRACT

The increasing presence of 1,1,1,2-tetrafluoroethane (CF_3CH_2F) in the atmosphere has prompted detailed studies into its complex photodissociation behavior. Experiments focusing on CF_3CH_2F irradiation have unveiled an array of ions, with the persistent observation of the rearrangement product CHF_2^+ not yet fully understood. In this work, we combine density functional theory, coupled-cluster calculations with a complete basis set formalism, and atom-centered density matrix propagation molecular dynamics to investigate the energetics and dynamics of different potential pathways leading to CHF_2^+. We found that the two-body dissociation pathway involving an HF rearrangement, which was previously considered complex for CHF_2^+ formation, is actually straightforward but not likely due to the facile loss of HF. In contrast, our calculations reveal that the H elimination pathway, once thought of as a potential route to CHF_2^+, is not only comparably disadvantageous from both thermodynamic and kinetic points of view but also does not align with experimental data, particularly the lack of a rebound peak at m/z 101–102. We establish that the formation of CHF_2^+ is predominantly via the HF elimination channel, a conclusion experimentally corroborated by studies involving the trifluoroethylene cation CF_2CHF^+, a key intermediate in this process.

I. INTRODUCTION

Among refrigerant gases, the 1,1,1,2-tetrafluoroethane (CF_3CH_2F) molecule, also known as R-134a, deserves special attention. Introduced to replace R-12 (dichlorodifluoromethane, CCl_2F_2), it has become the most abundant hydrofluorocarbon (HFC) in the atmosphere, as reported by Harrison *et al.*[1] Since the beginning of its commercial usage, CF_3CH_2F has been the subject of numerous experimental studies concerning the effects of ionizing radiation.[2–11] With a few exceptions,[10,11] most of them focused on valence ionization (more details on other CF_3CH_2F irradiation experiments are given elsewhere[11]). In the realm of computational studies centered on R-134a, a substantial body of research has also emerged,[12–17] the most recent of which is by our group.[17] There, we specifically examined the HF elimination from neutral and ionized R-134a and concluded that the most likely mechanism underpinning this reaction is a 2,1-HF elimination. This finding is consistent with the observations made for analogous HFCs, substantiated by both experimental and theoretical data.[18] Thus, considering the dominant mechanism only, both neutral and ionized HF eliminations follow a "four-centered" reaction pathway, as each atom within the main product originates from a different

C atom. The global reactions for these two 2,1-HF eliminations are listed below:

$$CF_3CH_2F \rightarrow HF + CF_2CHF, \quad (1)$$

$$CF_3CH_2F \rightarrow HF + CF_2CHF^+ + e^-. \quad (2)$$

According to our previous HF elimination study,[17] reaction (2) demands a substantial energy input of 308.7 kcal/mol, or 13.39 eV, at 0 K. This energy requirement is significantly higher than any activation energy observed for neutral processes. On the other hand, it only slightly surpasses the energy needed to produce the first photofragments detected in threshold photoelectron spectroscopy experiments.[4] In their study, carried out at 298 K, Zhou *et al.* initially detected CH_2F^+ at 12.99 ± 0.05 eV and, subsequently, CF_3^+ at 13.12 ± 0.05 eV, following the corresponding reactions:

$$CF_3CH_2F \rightarrow CF_3 + CH_2F^+ + e^-, \quad (3)$$

$$CF_3CH_2F \rightarrow CH_2F + CF_3^+ + e^-. \quad (4)$$

These two photofragments originate from the direct fragmentation of CF_3CH_2F upon ionization. Similarly, the subsequent ion detected with increased energy input, $CF_2CH_2F^+$,[19] also originates from the direct fragmentation of the parent species. However, some of the detected ions can only be generated through rearrangement reactions. A notable example is CHF_2^+,[4–8] which is commonly observed in these experiments and cannot be formed via direct fragmentation of ionized CF_3CH_2F. Interestingly, this rearrangement product ion is very often reported as the fourth most intense in mass spectra.[6] Following the investigation of Zhou *et al.*,[4] the detection of CHF_2^+ was also discussed by Kettunen *et al.*[5] and Morcelle *et al.*[7] in photoionization experiments, as well as by Majima *et al.*[6] and Pereira-da-Silva *et al.*[8] when using energetic C^+ ions and electrons, respectively. Although there is a consensus in the literature that molecular rearrangement is involved in CHF_2^+ formation, the specific mechanistic route is still a matter of debate. Initially, "H-atom migration" was proposed by Zhou *et al.*,[4] while other conjectures included "fluorine donation"[8] or a recombination reaction.[7] In any case, it is evident from previous studies that the pathway leading to CHF_2^+ formation remains an unresolved question.

We have selected a set of reactions associated with the production of CHF_2^+ based on suggestions from Zhou *et al.*[4] and listed them as follows:

$$CF_3CH_2F \rightarrow CHF_2 + CHF_2^+ + e^-, \quad (5)$$

$$CF_3CH_2F \rightarrow CF + HF + CHF_2^+ + e^-, \quad (6)$$

$$CF_3CH_2F \rightarrow H + CF_2 + CHF_2^+ + e^-, \quad (7)$$

$$CF_3CH_2F \rightarrow F + CHF + CHF_2^+ + e^-, \quad (8)$$

$$CF_3CH_2F \rightarrow F_2 + CH + CHF_2^+ + e^-. \quad (9)$$

In this work, we explore the energetic and dynamic aspects of various potential routes that can result in the formation of CHF_2^+. To accomplish this, we utilize density functional theory (DFT), coupled-cluster singles doubles perturbative triples [CCSD(T)] calculations employing a complete basis set formalism, and *ab initio* molecular dynamics. Our goal is to acquire a thorough understanding of the potential energy landscape, encompassing the distinct pathways proposed for CHF_2^+ formation. By employing a highly accurate computational protocol, we aim to elucidate the underlying rearrangement mechanism(s) at play in this chemical transformation.

II. METHODS

All chemical species have been fully optimized to attain their equilibrium geometries, with no imposition of any geometric constraints. These structures were evaluated as either minima or saddle points in the potential energy surface (PES) via harmonic vibrational frequency analysis. No scaling factor was used to correct the harmonic frequencies. Each optimized transition state (TS) structure was verified as the definitive saddle point in the minimum energy path connecting the two adjacent minima through intrinsic reaction coordinate (IRC) calculations.[20] Thermal energy and zero-point vibrational energy corrections have been incorporated into all energy results, which are expressed as enthalpies at 298.15 K. All geometry optimizations and vibrational frequency analyses were performed at the M06-2X[21]/cc-pVTZ[22] level of theory. As demonstrated in a previous study by our group,[17] this level is enough to obtain good quality geometries for fluoroalkanes and their corresponding cations.

We also performed coupled-cluster calculations—via the domain-based local pair natural orbital formalism, DLPNO-CCSD(T)—on each optimized geometry with tight SCF convergence criteria and the resolution of the identity with chain of spheres (RIJCOSX) approximation.[23–27] We opted for the DLPNO approach over the traditional one based on our preliminary benchmark calculations, which showed that both methods yield remarkably similar results, with the added advantage of the DLPNO approach being significantly faster (see the supplementary material for more details). To enhance the accuracy of our results toward the complete basis set (CBS) limit, we employed two basis sets, specifically cc-pVTZ and cc-pVQZ, and extrapolated toward the CBS limit using a power-law approach,[28,29]

$$E_{CBS} = E_{QZ} + \quad E_{QZ} - E_{TZ} \quad \frac{4^4}{5^4 - 4^4}. \quad (10)$$

In Eq. (10), E_{CBS} is the desired energy in the limit of an infinite basis set; E_{QZ} and E_{TZ} denote the energy of the system calculated with the finite basis sets, respectively, the quadruple-ζ (cc-pVQZ) and the triple-ζ (cc-pVTZ) basis sets. This extrapolation technique is rooted in the approaches proposed by distinct authors.[30–32] Atom-centered density matrix propagation (ADMP)[33–36] molecular dynamics simulations were performed for selected stationary points using the same level of theory as the geometry optimizations (M06-2X/cc-pVTZ). These primarily served to assess the HF rearrangement/elimination pathways, particularly focusing on the dynamic behavior of the ion–dipole structure $[CF_2CHF \cdots HF]^+$,[17] which constitutes the global minimum energy structure with the

FIG. 1. Schematic diagram for selected reaction pathways available from CF_3CH_2F photoionization with photon energy below 20 eV, as calculated at the DLPNO-CCSD(T)/CBS//M06-2X/cc-pVTZ level of theory. The numbers in the figure legend correspond to the numerical labels of the respective reactions.

formula $C_2H_2F_4^+$ (see the supplementary material for more information). We also carried out ADMP calculations starting from **TS1**, the transition state linking $CF_3CH_2F^+$ to the ion–dipole complex $[CF_2CHF \cdots HF]^+$ (see Fig. 1 for more details). The simulations were executed considering fully converged, self-consistent field wave functions at each time step. The initial nuclear kinetic energy (NKE) was varied over a range of values, namely 0.27, 0.50, 0.81, 1.08, 1.36, 1.63, 1.90, 2.17, 2.44, and 2.72 eV. We conducted simulations for each NKE value, with each simulation running for a total duration of 10 ps. The target temperature for the nuclear motion of the whole system was set to 298 K. In the ADMP approach, artificial masses are automatically assigned to the electronic degrees of freedom,[35] and these values can be sufficiently low to avoid the need for thermostats to ensure effective energy conservation. We monitored specific bond distances, with particular attention to the C–F bond involving the fluorine atom that is released as HF, throughout the entire duration of the simulations. All DLPNO-based coupled-cluster calculations were executed using Orca 5.0.3,[37,38] whereas all other calculations were carried out using the Gaussian 16, Revision A.03 package.[39]

III. RESULTS AND DISCUSSION

A. Assessment of the level of theory

Initially, we assessed the accuracy of the methods employed for calculating the thermochemical parameters of the reactions under investigation. To do so, the changes in enthalpy (ΔH) for reactions (1) and (3)–(8) are compared to the most accurate values reported in the existing literature. These ΔH comparisons were made at 298.15 K, herein referred to as ΔH_{298}. To calculate these values, we utilized the standard enthalpies of formation $\Delta_f H_{298}{}^\circ$ data for each chemical species, which were sourced from the works of Ganyecz *et al.*[40] for R-134a and Harvey *et al.*[41] for CHF_2 and CHF_2^+. In addition, we obtained data from the Active Thermochemical Tables (ATcT) database (version 1.124) when applicable.[42–47] The comparisons between our ΔH_{298} values and those from the literature are provided in kcal/mol in Table S1 and eV in Table S2. We included reaction (1), namely, the HF elimination from R-134a, for benchmarking purposes only. As shown in Table S1, the deviation from the reference value for reaction (1) at the CCSD(T)/CBS level is less than 0.1 kcal/mol (≈0.004 eV). This deviation is □10 times smaller than that observed in our previous HF elimination study.[17] Nevertheless, direct comparisons are not so straightforward, since here we changed both the reference for the $\Delta_f H_{298}{}^\circ$ of R-134a and the way of expressing thermochemistry results (ΔH_{298} instead of ΔE at 0 K).

Considering both coupled-cluster approaches, our results give ΔHs closely similar to the reference values, with a mean absolute deviation (MAD) <0.5 kcal/mol. The magnitude of deviations at the DLPNO-CCSD(T)/CBS level strongly resembles that of the traditional approach. However, in nearly all selected reactions, the sign of the deviation using DLPNO-CCSD(T) is opposite to that obtained with the conventional approach.

The sole exception to the sub-kcal/mol deviation is reaction (6), which leads to the formation of a CF radical. Nevertheless, the deviation of □1 kcal/mol for this reaction does not outweigh the fact that the average deviation of the coupled-cluster results remains lower than the average uncertainty for the best estimate values, which is 0.6 kcal/mol. For all other reactions, each predicted ΔH value at the DLPNO-CCSD(T)/CBS//M06-2X/cc-pVTZ level exhibits smaller errors when compared to the uncertainties associated with the reference values. Furthermore, the utilization of the DLPNO approach in coupled-cluster calculations has proven to be way faster than the conventional ones, as stated above. In addition, it has been demonstrated that DLPNO energies tend to be more accurate for smaller systems.[48] For these reasons, all energy results discussed hereafter are based on the DLPNO-CCSD(T)/CBS//M06-2X/cc-pVTZ level of theory.

From these benchmark calculations, we can reasonably infer a similar degree of confidence for other reactions involving analogous chemical species, i.e., both ionic and neutral fragments originating from CF_3CH_2F photoionization. Even though the results at the M06-2X/cc-pVTZ level reached an MAD approximately five times greater, their deviations still remain below 0.5 kcal/mol for reactions (3)–(5). This consistent performance, coupled with the previously attested reliability of M06-2X geometries,[17] has motivated us to proceed with the ADMP simulations, which we have performed at the same level of theory.

B. Thermochemistry analysis and mechanisms

Starting from the CHF_2^+ formation pathways listed above (5)–(8), we have thoroughly investigated these routes and identified new intermediates closely associated with CHF_2^+ production. Our main results are summarized in Fig. 1, focusing specifically on the cases associated with reactions (5)–(7). The set of reactions corresponding to the CHF_2^+ formation pathway from reactions (8) and (9) have not been considered in this analysis, as the final energy of the products exceeds the experimental threshold (see Table I) observed in the experiments by Zhou *et al.*[4] In Fig. 1, all energy values are referenced to those of neutral CF_3CH_2F. The diagram initiates with the singly ionized $CF_3CH_2F^+$ radical cation, which has a doublet ground state and whose adiabatic ionization energy is calculated as 12.30 eV. A remarkable structural feature of this system is the pronounced carbon–carbon bond length elongation

TABLE I. Comparison between the appearance energies (AEs) as obtained from Zhou *et al.*[4] and our computed ΔH_{298} values considering the reaction label given in the last column. TPEPICO stands for threshold photoelectron–photoion coincidence spectroscopy. Energy values are given in eV. Calculations are at the DLPNO-CCSD(T)/CBS//M06-2X/cc-pVTZ level of theory. Mean deviation: −0.29 ± 0.07 eV, considering only reactions (3), (4), and (11).

TPEPICO data from Zhou *et al.*[4]			This work	
			DLPNO-CCSD(T)/CBS	
Ion detected	Appearance energy (AE)	Reaction label	ΔH_{298}	Deviation
$CF_3CH_2F^+$	12.64 ± 0.05	(11)	12.30	−0.34
CH_2F^+	12.99 ± 0.05	(3)	13.31	−0.32
CF_3^+	13.12 ± 0.05	(4)	13.34	−0.22
CHF_2^+	16.11 ± 0.07	(5)	13.11	−3.00
		(6)	15.31	−0.80
		(7)	15.86	−0.25
		(8)	17.98	+1.87
		(9)	21.85	+5.74

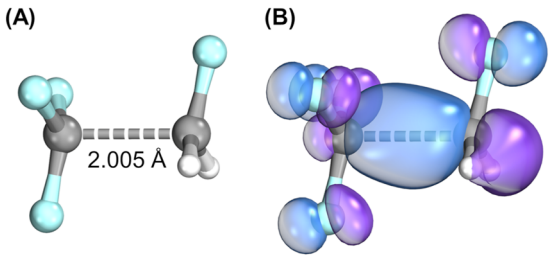

FIG. 2. (a) Optimized geometry of $CF_3CH_2F^+$ at the M06-2X/cc-pVTZ level of theory. The C–C bond length value is also shown. (b) IBO of $CF_3CH_2F^+$ depicting its 2c, 1e C–C σ bond.

to 2.005 Å [see Fig. 2(a)], 0.494 Å larger than that of the neutral system (1.511 Å). This distance falls within the range of other computed alkane radical cations[49,50] and is attributed to the formation of a two-center, one-electron (2c, 1e) C–C σ bond resulting from the valence ionization of CF_3CH_2F. Indeed, inspection of the intrinsic bond orbitals (IBOs)[51] of $CF_3CH_2F^+$ reveals the formation of such a one-electron bond, as highlighted in Fig. 2. In turn, Fig. 3 shows the molecular structures of key intermediates and transition states discussed in Fig. 1.

As illustrated in Fig. 1, the CHF_2^+ formation process within each investigated channel involves several distinct elementary steps. In accordance with the figure, each of the proposed elementary reactions shown is further detailed below, accompanied by the corresponding ΔH_{298} values [DLPNO-CCSD(T)/CBS//M06-2X/cc-pVTZ]:

HF rearrangement pathway,

$$CF_3CH_2F \rightarrow CF_3CH_2F^+ + e^- \quad \Delta H_{298} = 12.30 \text{ eV}, \tag{11}$$

$$CF_3CH_2F^+ \rightarrow CF_2CHF\cdots HF^+ \quad \Delta H_{298} = -1.18 \text{ eV}, \tag{12}$$

$$CF_2CHF\cdots HF^+ \rightarrow CHF_2CHF_2^+ \quad \Delta H_{298} = 0.97 \text{ eV}, \tag{13}$$

$$CHF_2CHF_2^+ \rightarrow CHF_2 + CHF_2^+ \quad \Delta H_{298} = 1.02 \text{ eV}. \tag{14}$$

HF elimination pathway, in addition to (11)–(13),

$$CF_2CHF\cdots HF^+ \rightarrow HF + CF_2CHF^+ \quad \Delta H_{298} = 0.46 \text{ eV}, \tag{15}$$

$$CF_2CHF^+ \rightarrow CFCHF_2^+ \quad \Delta H_{298} = 2.28 \text{ eV}, \tag{16}$$

$$CFCHF_2^+ \rightarrow CF + CHF_2^+ \quad \Delta H_{298} = 1.44 \text{ eV}. \tag{17}$$

H elimination pathway, in addition to (11),

$$CF_3CH_2F^+ \rightarrow H + CF_3CHF^+ \quad \Delta H_{298} = 1.85 \text{ eV}, \tag{18}$$

$$CF_3CHF^+ \rightarrow CF_2CHF_2^+ \quad \Delta H_{298} = -0.39 \text{ eV}, \tag{19}$$

$$CF_2CHF_2^+ \rightarrow CF_2\cdots CHF_2^+ \quad \Delta H_{298} = 1.59 \text{ eV}, \tag{20}$$

$$CF_2\cdots CHF_2^+ \rightarrow CF_2 + CHF_2^+ \quad \Delta H_{298} = 0.52 \text{ eV}. \tag{21}$$

From a thermodynamic standpoint, the HF rearrangement pathway, highlighted in red in Fig. 1, stands out as highly favorable. This is because, in contrast to the other pathways, it results in the formation of only two dissociation products, as opposed to three in all other cases. Notably, the enthalpy of the resulting products, $CHF_2 + CHF_2^+$, is only 0.81 eV above that of the singly charged $CF_3CH_2F^+$ at the DLPNO-CCSD(T)/CBS level, which is considerably lower than the enthalpy differences observed in the other channels. However, it is crucial to emphasize that this thermodynamic preference does not necessarily imply that this pathway is responsible for the CHF_2^+ production observed in the experiments.

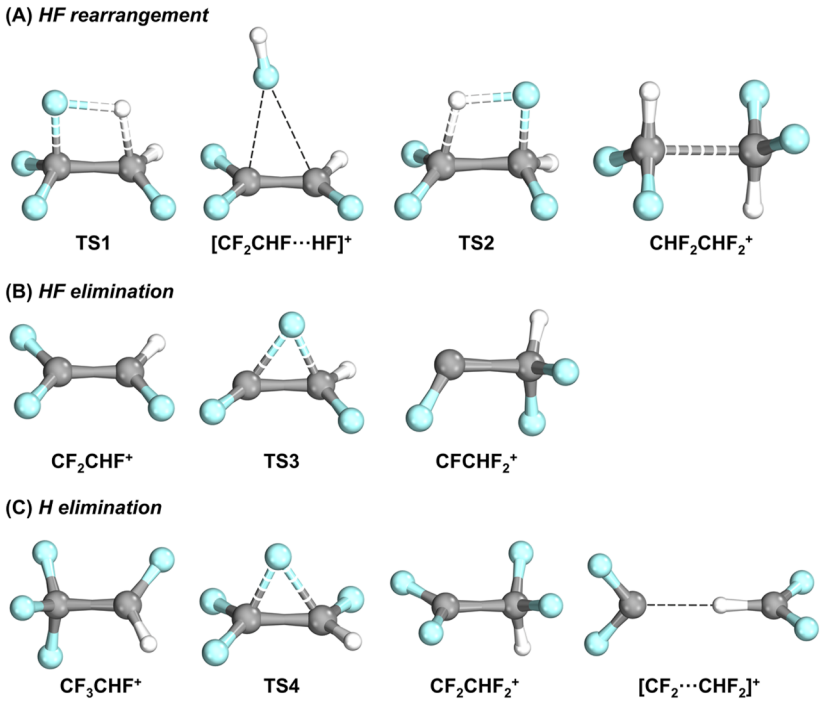

FIG. 3. 3D optimized structures (M06-2X/cc-pVTZ) of selected intermediates and transition states within the three investigated mechanistic pathways.

The initial step of the HF rearrangement (red curve) and the HF elimination (black curve) pathways involves the formation of the ion–dipole complex $[CF_2CHF\cdots HF]^+$, characterized by an energy barrier of 1.06 eV associated with **TS1**. Remarkably, this species represents the global minimum energy structure with the formula $C_2H_2F_4^+$. Our confidence in this claim was reinforced after conducting an exploratory search for stable $C_2H_2F_4^+$ geometries, which provided the same conclusion (more details are given in Sec. S2 of the supplementary material). Its structure is defined by an HF molecule nearly perpendicular to the CF_2CHF^+ core, where the F atom of HF is oriented toward the other fragment, and the C–F distances measure 2.444 and 2.646 Å at the M06-2X/cc-pVTZ level of theory.

From $[CF_2CHF\cdots HF]^+$, we identified **TS2**, which leads to an isomerization of the molecular ion from $CF_3CH_2F^+$ to $CHF_2CHF_2^+$. Notably, this isomerization has an energy barrier of 2.47 eV, which is nearly six times higher than the ΔH_{298} value for the competitive $[CF_2CHF\cdots HF]^+$ ion–dipole complex dissociation to form CF_2CHF^+ (ΔH_{298} = 0.46 eV). Given this substantial disparity in ΔH_{298} values between the two processes, it is conceivable that the elimination of HF from the ion–dipole adduct is considerably preferred, effectively impeding the system from progressing through **TS2**.

Regarding the HF elimination pathway (black curve), the subsequent step following the release of the HF molecule and the formation of CF_2CHF^+ is the fluorine atom migration from the CF_2 motif to CHF. This process is governed by **TS3** and is characterized by a notable energy barrier of 2.61 eV.[52] Interestingly, the enthalpy barrier for this migration step surpasses even the cumulative enthalpy cost of the initial and final steps of this pathway, which totals 2.50 eV. Despite this significant energy barrier, the isomerization of CF_2CHF^+ into $CFCHF_2^+$ is still energetically more favorable than the direct dissociation into CF_2 + CHF^+ (ΔH_{298} = 5.97 eV) or CF_2^+ + CHF (ΔH_{298} = 3.73 eV). The reason for these high-energy dissociation channels can be attributed to the breaking of a 2c, 2e C–C σ bond and a 2c, 1e C–C π bond [as illustrated in Fig. 4(a)].

In contrast, the dissociation of the C–C bond in $CFCHF_2^+$ is notably less energy-demanding, requiring 1.44 eV. In this case, the breakage involves only a 2c, 2e C–C σ bond since the unpaired electron in $CFCHF_2^+$ is associated with a non-bonding orbital

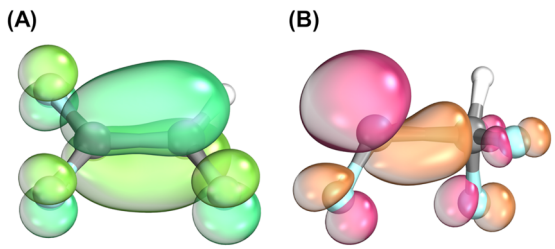

FIG. 4. (a) IBO of CF_2CHF^+, illustrating its 2c, 1e C–C π bond. (b) IBO of $CFCHF_2^+$, depicting that the unpaired electron is localized on a non-bonding orbital of the low-valent carbon atom.

of the low-valent carbon atom [as depicted in Fig. 4(b)]. Consequently, the formation of CHF_2^+ through the HF elimination pathway is the most feasible product following C–C bond dissociation. Here, CHF_2^+ is formed at a ΔH_{298} value of 15.31 eV from neutral CF_3CH_2F and, therefore, 2.20 eV higher than the value of the HF rearrangement pathway. Taking into account the observed experimental appearance energy (AE) of CHF_2^+ (16.11 eV),[4] which represents the minimum energy necessary in the experiment to detect this ion in the spectrum, our calculated value remains well within an acceptable range. In addition, our computational analysis supports this pathway as the most viable route for CHF_2^+ formation following the valence ionization of R-134a.

Differently from the other two pathways previously discussed, the H elimination pathway (depicted in blue in Fig. 1) has an entry thermodynamic barrier of ΔH_{298} = 1.85 eV, which is 0.79 eV higher than **TS1** and 0.84 eV higher than the direct dissociation of $CF_3CH_2F^+$ into CF_3 and CH_2F^+. Following the formation of CF_3CHF^+ after hydrogen detachment, the pathway continues with a fluorine migration from CF_3CHF^+ to $CF_2CHF_2^+$, a process that is notably exothermic, with an associated barrier [**TS4**, see Fig. 3(c)] of merely 0.27 eV.

The next step is the C–C bond dissociation of $CF_2CHF_2^+$. The process begins with the formation of an ion–dipole complex of the type $[CF_2 \cdots CHF_2]^+$ (ΔH_{298} = 1.59 eV). Inspection of its geometry [see Fig. 3(c)] clearly shows that the C–H bond of the CHF_2 motif is oriented toward the carbon atom of CF_2. However, it is important to highlight that the system may not necessarily have sufficient time to relax from a rotationally excited state to form this direction-oriented complex and might fully dissociate directly from $CF_2CHF_2^+$ to CF_2 and CHF_2^+, a process that possesses a ΔH_{298} value of 2.10 eV.

The final step of the H elimination pathway is the dissociation of $[CF_2 \cdots CHF_2]^+$ into isolated CF_2 and CHF_2^+ (ΔH_{298} = 0.51 eV). Notably, the CF_2 carbene is assumed to be formed (and eliminated) in the singlet state, as the energy difference between singlet and triplet states exceeds 2 eV.[53] The computed ΔH_{298} value for this step is greater than that for the HF elimination from $[CF_2CHF \cdots HF]^+$ (ΔH_{298} = 0.46 eV).

In light of the significant hindrance encountered by the HF rearrangement pathway, primarily driven by the favorability of HF elimination from $[CF_2CHF \cdots HF]^+$, we have identified two distinctive channels capable of yielding the rearrangement fragment CHF_2^+ following the valence ionization of CF_3CH_2F. These pathways are delineated by varying entry energy barriers. One exhibits a relatively lower energy barrier of 1.06 eV, associated with the HF elimination pathway, while the other, linked to H elimination, presents a higher thermodynamic barrier of 1.85 eV.

Moreover, when considering the latter pathway, direct dissociation from CF_3CHF^+ into either CF_3 and CHF^+ (ΔH_{298} = 4.30 eV) or alternatively CF_3^+ and CHF (ΔH_{298} = 3.29 eV) is found to be more endothermic compared to fluorine migration leading to $CF_2CHF_2^+$ (ΔH_{298} = −0.39 eV; barrier of 0.27 eV) and its subsequent dissociation into CF_2 and CHF_2^+ (ΔH_{298} = 2.10 eV). Similarly, as previously discussed, in the case of the HF elimination pathway, direct dissociation of the intermediate CF_2CHF^+ into either CF_2 and CHF^+ (ΔH_{298} = 5.97 eV) or, alternatively, CF_2^+ and CHF (ΔH_{298} = 3.73 eV) is more endothermic when compared to fluorine migration leading to $CFCHF_2^+$ (ΔH_{298} = 2.29 eV; barrier of 2.61 eV) and its subsequent dissociation into CF and CHF_2^+ (ΔH_{298} = 1.44 eV).

In essence, both pathways reveal that an atom migration step followed by C–C dissociation is kinetically and thermodynamically preferred over direct dissociation into non-rearranged fragments. To determine which pathway actively leads to the production of CHF_2^+, three key factors must be considered. First, our calculations indicate that the H elimination step from the parent ion occurs without a reverse barrier. Second, the fragment ion of m/z = 101, the product of H elimination, should be stable over a range of around 1.7 eV. Third, limitations in the mass resolution of the experiments conducted by Zhou *et al.*[4] resulted in overlapping signals of CF_3CHF^+ (m/z = 101) and the parent ion $CF_3CH_2F^+$ (m/z = 102). Collectively, these considerations indicate that should the H elimination pathway be active, an increase in signal within the m/z 101–102 mass range across a broad energy spectrum is anticipated. This signal rebound would be attributed to the indistinct presence of CF_3CHF^+, which would become the prevailing signal as the one from the parent ion diminishes. Contrarily, experimental evidence from Zhou *et al.*[4] demonstrates a rapid decline in the peak within this m/z range in the coincidence yields. This absence of rebound in the experimental data, when considered in conjunction with our calculations, strongly suggests that the H elimination pathway is not a significant competitor in the formation of CHF_2^+, thereby diminishing its likelihood as a contributing mechanism. Consequently, it is reasonable to conclude that the CHF_2^+ formation is most likely driven by the pathway involving the elimination of HF.

Additional support for the formation of CHF_2^+ through HF elimination is found in the research by Harvey *et al.*,[54] which investigates the fragmentation of ionized trifluoroethane, CF_2CHF^+. In our study, this molecule was identified as a pivotal intermediate in the HF elimination pathway. Harvey *et al.*[54] reported that the primary daughter ion produced from CF_2CHF^+ is CHF_2^+, indicative of the loss of a CF fragment, a process that necessitates an initial migration of an F atom. Our computational reaction pathway starting from CF_2CHF^+, outlined in Fig. 1, is in excellent agreement with their proposed mechanism, offering a convincing explanation for the experimental observations related to CHF_2^+ formation from $CF_3CH_2F^+$. It is important to note, however, that the experiments by Zhou *et al.*[4] did not observe the precise detection of CF_2CHF^+, probably due to insufficient mass resolution. Therefore, conducting new experiments with enhanced resolution is essential to conclusively determining the dominant pathway contributing to the rearrangement product.

In Table I, we present the energetics of dissociative photoionization pathways of CF_3CH_2F at 298.15 K, as measured in the work of Zhou *et al.*[4] These values are then compared with the results obtained through the calculations conducted herein. It is important to note that Zhou *et al.*[4] reported appearance energies, and to ensure an accurate correspondence, we meticulously cross-referenced each of the studied reactions with the specific process responsible for the detection of each ion. In Table I, we also included a comparison between the AE of $CF_3CH_2F^+$ as estimated by Zhou *et al.*[4] (12.64 eV) and our calculated ΔH_{298} value (12.30 eV) for the adiabatic ionization reaction.

For reactions (3) and (4), where the primary ion formation occurs through direct dissociation of the C–C bond in $CF_3CH_2F^+$,

our calculated ΔH_{298} values show a deviation compared to the experimentally obtained AE of −0.32 and −0.22 eV, respectively. The negative signs indicate that the ΔH_{298} values are smaller than the corresponding AEs. When we consider these deviations along with reaction (11), the average deviation amounts to −0.29 ± 0.07 eV.

Table I also presents the AE of CHF_2^+ (16.11 eV) and compares it with the formation of CHF_2^+ according to reactions (5)–(9). As anticipated, the HF rearrangement reaction (5) exhibits a very small ΔH_{298} value (13.11 eV), but this pathway is hindered by the facile HF elimination. In contrast, reactions (8) and (9) have ΔH_{298} values of 17.98 and 21.85 eV, with deviations of +1.87 and +5.74 eV compared to the AE of CHF_2^+. These high values underscore their unsuitability as potential pathways for CHF_2^+ formation under the experimental conditions.

Finally, reactions (6) and (7), representing the HF elimination and H elimination pathways, respectively, exhibit values that align more closely with the AE of CHF_2^+, with deviations of −0.80 and −0.25 eV, respectively. These results indicate that both channels could potentially contribute to the observation of CHF_2^+ resulting from the valence ionization of CF_3CH_2F. Although there is better agreement between the AE of CHF_2^+ and the ΔH_{298} value of the H elimination channel, this finding does not contradict our previous conclusions. Other factors, aside from the reaction energy, can influence the AE value. Therefore, while ΔH_{298} values can help discard channels with energy levels that are either too low or too high, those with ΔH values closer to the AE value cannot be ruled out, even if one appears to align more closely. A parallel line of reasoning is also evident in the work of Zhou *et al.*[4]

By using the results from the DLPNO-CCSD(T)/CBS//M06-2X/cc-pVTZ calculations, as shown in Table I, we can gain insights into other experimental findings related to the photoionization of CF_3CH_2F, particularly in the context of F atom elimination,

$$CF_3CH_2F \rightarrow F + CF_2CH_2F^+ + e^-. \tag{22}$$

In the photoionization study by Zhou *et al.*,[4] the reaction depicted in (22) was also examined, with a particular focus on the formation of $CF_2CH_2F^+$ as a product of F loss. The authors measured an appearance energy (AE) of 15.07 ± 0.07 eV for this ion, presuming it to be the exclusive result of F elimination. In contrast, our calculations indicate that the F elimination reaction has a ΔH_{298} of 13.85 eV, relative to the energy of the ground state of neutral CF_3CH_2F. This leads to a calculated AE value of 14.13 ± 0.07 eV, assuming that the kinetic energy release (KER) for this reaction is consistent with that observed for other main fragments in the same study.

Therefore, it can be inferred that the process of fluorine loss is accompanied by a high KER of □1 eV. This observation was indeed corroborated by Zhou *et al.*[4] It is noteworthy that this finding is analogous to phenomena observed in the fragmentation of multiple halogenated hydrocarbons, where non-statistical losses of halogen atoms from electronically excited cation states were reported. These processes can result in a fragment ion appearing at an energy significantly higher than its thermodynamic threshold.[54–56] This mechanism could potentially account for the unexpectedly high KER observed for fluorine loss in Zhou's experiments, suggesting a more complex interplay of factors beyond ground-state dynamics in the formation of $CF_2CH_2F^+$.

C. ADMP results

Now, we direct our attention to $[CF_2CHF\cdots HF]^+$, representing the global minimum structure with a $C_2H_2F_4^+$ stoichiometry, and **TS1**, the transitional state that connects this global minimum structure to the singly charged $CF_3CH_2F^+$ species. As previously mentioned, the HF rearrangement pathway faces a challenge due to the existence of a low-energy pathway associated with the release of the HF molecule from the global minimum. Notably, ions exhibiting the $C_2H_2F_4^+$ stoichiometry are commonly observed in the threshold photoelectron experiments that served as the motivation for the present study.[2] This led us to investigate whether these signals could, in part, be attributed to the global minimum structure.

This consideration gains significance when we acknowledge that the detection of ions, particularly in time-of-flight experiments, typically occurs within the microsecond timescale.[57] During this time, ions can undergo complete molecular rearrangement toward their respective global minimum energy structures if kinetic barriers are not substantial. It is worth noting that both the global minimum energy structure and the low-lying isomers of ionized molecules can significantly differ from their neutral counterparts.

A striking example is benzene (C_6H_6), where its singly charged version exhibits a $^2E_{1g}$ ground state in a D_{6h} geometry, which experiences a Jahn–Teller distortion to transition to a lower energy D_{2h} distorted structure.[58,59] Furthermore, the doubly charged global minimum of benzene is characterized by a pentagonal-pyramidal structure, a subject of interest in various experimental and theoretical investigations.[60–64] Similar structural variations depending on the charge state have been observed in other organic systems, encompassing hydrocarbons such as toluene ($C_6H_5CH_3$),[65–67] naphthalene ($C_{10}H_8$),[68] biphenyl ($C_{12}H_{10}$),[69] and phenanthrene,[70] as well as molecules featuring functional groups, including $C_2H_4O_2$ isomers,[71] halogen-containing compounds,[72–74] and pyrrole (C_4H_nN) derivatives.[75]

To assess the involvement of $[CF_2CHF\cdots HF]^+$ in the photoionization of R-134a, we carried out *ab initio* molecular dynamics simulations using the ADMP method, initiating from the $[CF_2CHF\cdots HF]^+$ and **TS1** configurations. These simulations were conducted at various nuclear kinetic energy (NKE) levels, as discussed earlier, and the results are summarized in Fig. 5.

Figure 5(a) illustrates a series of distinct trajectories, each corresponding to a specific NKE value, originating from the optimized $[CF_2CHF\cdots HF]^+$ structure. For our simulations, we deliberately selected one of the C–F bond distances, namely, the shortest one that encompasses the F atom from the HF motif and one of the C atoms from the CF_2CHF framework. This distance was closely monitored throughout the dynamics. As the initial structure is an ion–dipole, two dashed lines are included in the plot for reference: (i) representing a C–F bond length (1.72 Å) 30% larger than the sum of covalent radii,[76] and (ii) indicating the sum of van der Waals (vdW) radii (3.17 Å).

In Fig. 5(a), it is evident that the initial C–F distance falls between the reference values, as expected due to the ion–dipole nature of $[CF_2CHF\cdots HF]^+$. Up to an NKE value of 1.36 eV, there is only a slight variation in the C–F distance, indicating that the system maintains its stability for the first 600 fs. Beyond this time point, some larger oscillations in bond length are evident. However, in all cases, the maximum C–F distance remains below the sum of the van der Waals (vdW) radii.

In stark contrast, when examining dynamics associated with NKE values exceeding 1.36 eV, systematic oscillations in the C–F distance become apparent within the first few hundred femtoseconds. After 500 fs, more significant fluctuations in this structural property occur, with all trajectories for NKE values above 2.00 eV leading to C–F distances exceeding the sum of the vdW radii. Bond oscillations persist across all trajectories, even in the case of an NKE value of 2.17 eV, where the HF molecule is recaptured and the system returns to the equilibrium C–F distance of $[CF_2CHF\cdots HF]^+$ at ∼850 fs. However, in this trajectory, a new oscillation emerges, and after 100 fs, the system appears to be on the verge of complete dissociation.

For the two trajectories with the highest NKE values, specifically 2.44 and 2.72 eV, there is no observed return to C–F bond distances below the sum of the vdW radii, even though some oscillations in bond lengths persist after the dissociation point. Collectively, these findings suggest that, if $[CF_2CHF\cdots HF]^+$ is initially formed, moderate thermal effects can indeed trigger the elimination of HF.

Figure 5(b) illustrates the system's dynamics when starting from the **TS1** structure. In this case, the initial C–F distance is shorter than the sum of the covalent radii. In stark contrast to the previous scenario, it is evident that even for the lowest NKE value, HF is readily eliminated from the structure, occurring even before the 100 fs mark.

The time required for dissociation, i.e., the duration for the C–F distance to reach the reference value matching the sum of the vdW radii, is displayed in Fig. 5(c). The inspection of the figure shows that the dissociation time varies from 62 fs for an NKE value of 0.27 eV to 44 fs for an NKE value of 2.72 eV. These outcomes strongly indicate that the complex is not formed under the experimental conditions, despite it being the global minimum of the $C_2H_2F_4^+$ system. Furthermore, they point out the improbability of CHF_2^+ formation through a two-body dissociation channel, which would involve initial HF molecule rearrangement and subsequent C–C bond dissociation through the $CHF_2CHF_2^+$ isomer of singly charged R-134a. These findings not only align remarkably well with the prior works that have already indicated the thermodynamic incompatibility of this pathway with the measured appearance energies but also emphasize the prominent role played by the facile gas-phase elimination of HF in this context.

FIG. 5. ADMP dynamics starting from the (a) $[CF_2CHF\cdots HF]^+$ and (b) **TS1** optimized structures, with consideration of various average nuclear kinetic energies. The dynamics were tracked by monitoring a crucial C–F distance (see the text for details). The plots display the sum of the C and F vdW radii (3.17 Å) and a C–F distance 30% larger than the sum of covalent radii (1.72 Å) as reference points. (c) Time for dissociation as a function of the average nuclear kinetic energy, starting from the **TS1** geometry. All ADMP results are obtained at the M06-2X/cc-pVTZ level of theory.

IV. CONCLUSIONS

In summary, our detailed study aimed to thoroughly understand the photoionization of 1,1,1,2-tetrafluoroethane (CF_3CH_2F) and the puzzling formation of CHF_2^+ ions. Our approach, employing a combination of computational techniques, has shed light on the energetics and dynamics governing the various potential pathways leading to CHF_2^+ formation. Initially, the HF rearrangement pathway appeared thermodynamically attractive due to its lower reaction enthalpy and the production of only two dissociation products. However, this pathway is impeded by the facile elimination of HF, leading us to explore alternative routes for

CHF_2^+ formation. Notably, the F elimination pathway and the F_2 formation pathway proved thermodynamically too high in energy, leaving two remaining competitive pathways: H elimination and HF elimination.

Our analysis has unveiled three pivotal factors endorsing the HF elimination pathway. First, its entry energy is notably lower than that of H elimination, a trend that persists throughout the entire reaction mechanism. Second, the F migration step before CHF_2^+ formation in the HF elimination pathway is more favorable, both kinetically and thermodynamically, than direct C–C dissociation from the CF_2CHF^+ intermediate. This indicates that F migration precedes dissociation after CF_2CHF^+ formation, leading preferentially to the expected CHF_2^+ ion. Third, our findings indicate that the H elimination from the parent ion lacks a reverse barrier, and the dehydrogenated fragment is stable for about 1.7 eV. Considering that these results are expected to yield noticeable effects in the experiments, the absence of a rebound in the peak within the m/z 101–102 mass range supports the inactivity of this pathway over the photon energy range investigated herein. These considerations provide compelling evidence for HF elimination as the dominant mechanism for CHF_2^+ formation.

Finally, our molecular dynamics simulations demonstrated that the ion–dipole complex $[CF_2CHF\cdots HF]^+$, the global energy minimum of the $C_2H_2F_4^+$ system, is unlikely to form under experimental conditions due to the ready dissociation of HF from its precursor transition state. This reaffirms prior research highlighting the thermodynamic incompatibility of the HF rearrangement pathway with measured appearance energies. Taken together, our findings provide new insights into the complex dissociation pathways of R-134a, the most abundant hydrofluorocarbon present in Earth's atmosphere, following its valence ionization.

SUPPLEMENTARY MATERIAL

See the supplemetary material for additional details on data analysis and the Cartesian coordinates of all species.

ACKNOWLEDGMENTS

V.S.A.B., C.P.S., and F.F. acknowledge the University of Kent for providing financial and computational resources. Special thanks are extended to Dr. Timothy Kinnear for HPC assistance. All authors thank Professor Bernd Engels and Professor João B. L. Martins for providing additional computational resources. V.S.A.B., A.C.F.S., and F.F. acknowledge CNPq for a postdoctoral fellowship to V.S.A.B. (Grant Nos. 26/2021 and 401325/2022-9). V.S.A.B. thanks the National Institute of Science and Technology on Molecular Sciences (INCT-CiMol) for a postdoctoral fellowship (Grant No. CNPq 406804/2022-2). C.P.S. and F.F. thank the Engineering and Physical Sciences Research Council (EPSRC) for a Ph.D. studentship for C.P.S.

AUTHOR DECLARATIONS

Conflict of Interest

The authors have no conflicts to disclose.

Author Contributions

Víctor S. A. Bonfim: Conceptualization (equal); Formal analysis (equal); Investigation (equal); Methodology (equal); Writing – original draft (equal); Writing – review & editing (equal). **Cauê P. Souza**: Formal analysis (supporting); Investigation (supporting); Software (supporting); Validation (lead); Visualization (supporting); Writing – review & editing (supporting). **Daniel A. B. de Oliveira**: Formal analysis (equal); Investigation (equal); Methodology (equal); Writing – review & editing (supporting). **Leonardo Baptista**: Supervision (equal); Writing – review & editing (equal). **Antônio C. F. Santos**: Conceptualization (lead); Funding acquisition (lead); Project administration (equal); Supervision (equal); Writing – review & editing (supporting). **Felipe Fantuzzi**: Conceptualization (equal); Formal analysis (equal); Funding acquisition (equal); Investigation (supporting); Methodology (equal); Project administration (equal); Resources (lead); Software (lead); Supervision (equal); Visualization (lead); Writing – original draft (lead); Writing – review & editing (equal).

DATA AVAILABILITY

The data that support the findings of this study are available within the article and its supplementary material and from the corresponding author upon reasonable request.

REFERENCES

[1] J. J. Harrison, M. P. Chipperfield, C. D. Boone, S. S. Dhomse, and P. F. Bernath, "Fifteen years of HFC-134a satellite observations: Comparisons with SLIMCAT calculations," J. Geophys. Res.: Atmos. **126**(8), e2020JD033208, https://doi.org/10.1029/2020jd033208 (2021).

[2] A. Reizian, Y. Dat, S. Rault, and M. Robba, "Mass spectral study of chlorofluorocarbons (CFCs) and potential alternatives (HCFCs and HFCs)," Ecotoxicol. Environ. Saf. **29**(1), 47–60 (1994).

[3] A. Reizian-Fouley, Y. Dat, and S. Rault, "Chlorofluorocarbon CFCs, potential alternative HCFCs and HFCs, and related chlorinated compounds: Mass spectral study, Part II," Ecotoxicol. Environ. Saf. **36**(3), 197–204 (1997).

[4] W. Zhou, D. P. Seccombe, and R. P. Tuckett, "Fragmentation of valence electronic states of CF_3–CH_2F^+ and CHF_2–CHF_2^+ in the range 12–25 eV," Phys. Chem. Chem. Phys. **4**(19), 4623–4633 (2002).

[5] J. A. Kettunen, A. Sankari, L. Partanen, S. Urpelainen, A. Kivimäki, and M. Huttula, "Valence electronic structure and photofragmentation of 1,1,1,2-tetrafluoroethane (CF_3-CH_2F)," Phys. Rev. A **85**(6), 062703 (2012).

[6] T. Majima, T. Murai, S. Yoshida, M. Saito, H. Tsuchida, and A. Itoh, "Fragmentation of multiply ionized CF_3–CH_2F induced by charge-changing collisions with fast carbon ions," Int. J. Mass Spectrom. **421**, 25–32 (2017).

[7] V. Morcelle, A. Medina, L. C. Ribeiro, I. Prazeres, R. R. T. Marinho, M. S. Arruda, L. A. V. Mendes, M. J. Santos, B. N. C. Tenório, A. B. Rocha, and A. C. F. Santos, "Fragmentation of valence and carbon core excited and ionized CH_2FCF_3 molecule," J. Phys. Chem. A **122**(51), 9755–9760 (2018).

[8] J. Pereira-da-Silva, R. Rodrigues, J. Ramos, C. Brígido, A. Botnari, M. Silvestre, J. Ameixa, M. Mendes, F. Zappa, S. J. Mullock, J. M. M. Araújo, M. T. d. N. Varella, L. M. Cornetta, and F. F. da Silva, "Electron driven reactions in tetrafluoroethane: Positive and negative ion formation," J. Am. Soc. Mass Spectrom. **32**(6), 1459–1468 (2021).

[9] K. Okutsu, N. Saito, and H. Ohmura, "Investigation of dissociative photoionization pathways for orientation-selected molecules by phase-controlled laser fields," AIP Adv. **11**(1), 015246 (2021).

[10]V. Morcelle, A. Medina, L. C. Ribeiro, I. Prazeres, R. R. T. Marinho, M. S. Arruda, L. A. V. Mendes, M. d. J. Santos, and A. C. F. d. Santos, "Double-valence photoionization of SUVA134a molecule (CFH_2CF_3)," Rapid Commun. Mass Spectrom. **35**(16), e9132 (2021).
[11]V. S. A. Bonfim, I. Prazeres, V. Morcelle, R. R. T. Marinho, M. S. Arruda, L. A. V. Mendes, L. C. Ribeiro, M. J. Santos, A. Medina, and A. C. F. Santos, "1,1,1,2-tetrafluoroethane photofragmentation: A translational kinetic energy release analysis in the EUV and X-ray energies range," Mol. Phys. **120**(14), e2100836 (2022).
[12]J. M. Martell and R. J. Boyd, "An ab initio study of the series of fluorinated ethanes $C_2H_nF_{6-n}$ (n = 0–6): Geometries, total energies, and C–C bond dissociation energies," J. Phys. Chem. **96**(15), 6287–6290 (1992).
[13]K. Lucas, U. Delfs, V. Buss, and M. Speis, "Ideal-gas properties of new refrigerants from quantum mechanical ab initio calculations," Int. J. Thermophys. **14**(5), 993–1006 (1993).
[14]T. Yamada, T. H. Lay, and J. W. Bozzelli, "*Ab initio* calculations and internal rotor: Contribution for thermodynamic properties S°_{298} and $C_p(T)$'s (300 < T/K < 1500): Group additivity for fluoroethanes," J. Phys. Chem. A **102**(37), 7286–7293 (1998).
[15]T. M. Klapötke and J. M. Winfield, "The gas phase structure and acidity of the neutral Brønsted acid 1,1,1,2-tetrafluoroethane," J. Fluorine Chem. **88**(1), 19–22 (1998).
[16]T. Hayashi, K. Ishikawa, M. Sekine, and M. Hori, "Dissociative properties of 1,1,1,2-tetrafluoroethane obtained by computational chemistry," Jpn. J. Appl. Phys. **57**(6S2), 06JC02 (2018).
[17]V. S. A. Bonfim, L. Baptista, D. A. B. Oliveira, D. E. Honda, and A. C. F. Santos, "Kinetic and thermodynamic investigations on the HF elimination reactions from neutral and ionized CF_3CH_2F," J. Mol. Model. **28**(10), 309 (2022).
[18]C. A. Smith, B. R. Gillespie, G. L. Heard, D. W. Setser, and B. E. Holmes, "The unimolecular reactions of CF_3CHF_2 studied by chemical activation: Assignment of rate constants and threshold energies to the 1,2-H atom transfer, 1,1-HF and 1,2-HF elimination reactions, and the dependence of threshold energies on the number of F-atom substituents in the fluoroethane molecules," J. Phys. Chem. A **121**(46), 8746–8756 (2017).
[19]$CF_2CH_2F^+$ or any of its $C_2H_2F_3^+$ isomers with an m/z ratio of 83, as detection was confirmed by mass spectra.
[20]K. Fukui, "The path of chemical reactions–the IRC approach," Acc. Chem. Res. **14**(12), 363–368 (1981).
[21]Y. Zhao and D. G. Truhlar, "The M06 suite of density functionals for main group thermochemistry, thermochemical kinetics, noncovalent interactions, excited states, and transition elements: Two new functionals and systematic testing of four M06-class functionals and 12 other functionals," Theor. Chem. Acc. **120**(1–3), 215–241 (2008).
[22]T. H. Dunning, "Gaussian basis sets for use in correlated molecular calculations. I. The atoms boron through neon and hydrogen," J. Chem. Phys. **90**(2), 1007–1023 (1989).
[23]C. Riplinger, B. Sandhoefer, A. Hansen, and F. Neese, "Natural triple excitations in local coupled cluster calculations with pair natural orbitals," J. Chem. Phys. **139**(13), 134101 (2013).
[24]C. Riplinger and F. Neese, "An efficient and near linear scaling pair natural orbital based local coupled cluster method," J. Chem. Phys. **138**(3), 034106 (2013).
[25]C. Riplinger, P. Pinski, U. Becker, E. F. Valeev, and F. Neese, "Sparse maps—A systematic infrastructure for reduced-scaling electronic structure methods. II. Linear scaling domain based pair natural orbital coupled cluster theory," J. Chem. Phys. **144**(2), 024109 (2016).
[26]M. Saitow, U. Becker, C. Riplinger, E. F. Valeev, and F. Neese, "A new near-linear scaling, efficient and accurate, open-shell domain-based local pair natural orbital coupled cluster singles and doubles theory," J. Chem. Phys. **146**(16), 164105 (2017).
[27]Y. Guo, C. Riplinger, U. Becker, D. G. Liakos, Y. Minenkov, L. Cavallo, and F. Neese, "Communication: An improved linear scaling perturbative triples correction for the domain based local pair-natural orbital based singles and doubles coupled cluster method [DLPNO-CCSD(T)]," J. Chem. Phys. **148**(1), 011101 (2018).
[28]C. F. Goldsmith, S. J. Klippenstein, and W. H. Green, "Theoretical rate coefficients for allyl + HO_2 and allyloxy decomposition," Proc. Combust. Inst. **33**(1), 273–282 (2011).
[29]T. T. Pekkanen, R. S. Timonen, S. H. Robertson, G. Lendvay, S. P. Joshi, T. T. Reijonen, and A. J. Eskola, "An experimental and computational study of the reaction between 2-methylallyl radicals and oxygen molecules: Optimizing master equation parameters with trace fitting," Phys. Chem. Chem. Phys. **24**(8), 4729–4742 (2022).
[30]J. M. L. Martin, "Ab initio total atomization energies of small molecules–towards the basis set limit," Chem. Phys. Lett. **259**(5–6), 669–678 (1996).
[31]A. Halkier, T. Helgaker, P. Jørgensen, W. Klopper, H. Koch, J. Olsen, and A. K. Wilson, "Basis-set convergence in correlated calculations on Ne, N_2, and H_2O," Chem. Phys. Lett. **286**(3–4), 243–252 (1998).
[32]D. Feller and D. A. Dixon, "Extended benchmark studies of coupled cluster theory through triple excitations," J. Chem. Phys. **115**(8), 3484–3496 (2001).
[33]H. B. Schlegel, J. M. Millam, S. S. Iyengar, G. A. Voth, A. D. Daniels, G. E. Scuseria, and M. J. Frisch, "*Ab initio* molecular dynamics: Propagating the density matrix with Gaussian orbitals," J. Chem. Phys. **114**(22), 9758–9763 (2001).
[34]S. S. Iyengar, H. B. Schlegel, J. M. Millam, G. A. Voth, G. E. Scuseria, and M. J. Frisch, "*Ab initio* molecular dynamics: Propagating the density matrix with Gaussian orbitals. II. Generalizations based on mass-weighting, idempotency, energy conservation and choice of initial conditions," J. Chem. Phys. **115**(22), 10291–10302 (2001).
[35]H. B. Schlegel, S. S. Iyengar, X. Li, J. M. Millam, G. A. Voth, G. E. Scuseria, and M. J. Frisch, "*Ab initio* molecular dynamics: Propagating the density matrix with Gaussian orbitals. III. Comparison with Born–Oppenheimer dynamics," J. Chem. Phys. **117**(19), 8694–8704 (2002).
[36]S. S. Iyengar, H. B. Schlegel, and G. A. Voth, "Atom-centered density matrix propagation (ADMP): Generalizations using Bohmian mechanics," J. Phys. Chem. A **107**(37), 7269–7277 (2003).
[37]F. Neese, "The ORCA program system," Wiley Interdiscip. Rev.: Comput. Mol. Sci. **2**(1), 73–78 (2012).
[38]F. Neese, "Software update: The ORCA program system—Version 5.0," Wiley Interdiscip. Rev.: Comput. Mol. Sci. **12**(5), e1606 (2022).
[39]M. J. Frisch, G. W. Trucks, H. B. Schlegel, G. E. Scuseria, M. A. Robb, J. R. Cheeseman, G. Scalmani, V. Barone, B. Mennucci, G. A. Petersson, H. Nakatsuji, M. Caricato, X. Li, H. P. Hratchian, A. F. Izmaylov, J. Bloino, G. Zheng, J. L. Sonnenberg, M. Hada, M. Ehara, K. Toyota, R. Fukuda, J. Hasegawa, M. Ishida, T. Nakajima, Y. Honda, O. Kitao, H. Nakai, T. Vreven, J. A. Montgomery, Jr., J. E. Peralta, F. Ogliaro, M. Bearpark, J. J. Heyd, E. Brothers, K. N. Kudin, V. N. Staroverov, R. Kobayashi, J. Normand, K. Raghavachari, A. Rendell, J. C. Burant, S. S. Iyengar, J. Tomasi, M. Cossi, N. Rega, J. M. Millam, M. Klene, J. E. Knox, J. B. Cross, V. Bakken, C. Adamo, J. Jaramillo, R. Gomperts, R. E. Stratmann, O. Yazyev, A. J. Austin, R. Cammi, C. Pomelli, J. W. Ochterski, R. L. Martin, K. Morokuma, V. G. Zakrzewski, G. A. Voth, P. Salvador, J. J. Dannenberg, S. Dapprich, A. D. Daniels, Ö. Farkas, J. B. Foresman, J. V Ortiz, J. Cioslowski, and D. J. Fox, *Gaussian 16, Revision A.03*, Gaussian, Inc., Wallingford, CT, 2016.
[40]Á. Ganyecz, M. Kállay, and J. Csontos, "High accuracy quantum chemical and thermochemical network data for the heats of formation of fluorinated and chlorinated methanes and ethanes," J. Phys. Chem. A **122**(28), 5993–6006 (2018).
[41]J. Harvey, R. P. Tuckett, and A. Bodi, "A halomethane thermochemical network from iPEPICO experiments and quantum chemical calculations," J. Phys. Chem. A **116**(39), 9696–9705 (2012).
[42]B. Ruscic, R. E. Pinzon, M. L. Morton, G. von Laszevski, S. J. Bittner, S. G. Nijsure, K. A. Amin, M. Minkoff, and A. F. Wagner, "Introduction to active thermochemical tables: Several 'key' enthalpies of formation revisited," J. Phys. Chem. A **108**(45), 9979–9997 (2004).
[43]B. Ruscic, R. E. Pinzon, G. v. Laszewski, D. Kodeboyina, A. Burcat, D. Leahy, D. Montoy, and A. F. Wagner, "Active thermochemical tables: Thermochemistry for the 21st century," J. Phys.: Conf. Ser. **16**, 561–570 (2005).
[44]B. Ruscic, "Active thermochemical tables: Sequential bond dissociation enthalpies of methane, ethane, and methanol and the related thermochemistry," J. Phys. Chem. A **119**(28), 7810–7837 (2015).

[45] S. J. Klippenstein, L. B. Harding, and B. Ruscic, "Ab initio computations and active thermochemical tables hand in hand: Heats of formation of core combustion species," J. Phys. Chem. A **121**(35), 6580–6602 (2017).
[46] B. Ruscic, "Uncertainty quantification in thermochemistry, benchmarking electronic structure computations, and Active Thermochemical Tables," Int. J. Quantum Chem. **114**(17), 1097–1101 (2014).
[47] B. Ruscic and D. H. Bross, Active thermochemical tables (ATcT) values based on ver. 1.124 of the thermochemical network, Argonne National Laboratory, Lemont, IL, 2022, available at: ATcT.anl.gov.
[48] I. Sandler, J. Chen, M. Taylor, S. Sharma, and J. Ho, "Accuracy of DLPNO-CCSD(T): Effect of basis set and system size," J. Phys. Chem. A **125**(7), 1553–1563 (2021).
[49] T. E. Shubina and A. A. Fokin, "Hydrocarbon σ-radical cations," Wiley Interdiscip. Rev.: Comput. Mol. Sci. **1**(5), 661–679 (2011).
[50] F. Fantuzzi, W. Wolff, H. M. Quitián-Lara, H. M. Boechat-Roberty, G. Hilgers, B. Rudek, and M. A. C. Nascimento, "Unexpected reversal of stability in strained systems containing one-electron bonds," Phys. Chem. Chem. Phys. **21**(45), 24984–24992 (2019).
[51] G. Knizia, "Intrinsic atomic orbitals: An unbiased bridge between quantum theory and chemical concepts," J. Chem. Theory Comput. **9**(11), 4834–4843 (2013).
[52] A transition state for hydrogen atom migration from the CHF motif to CF_2 in CF_2CHF^+, namely **TS3′**, was also found. It lies at ΔH_{298} = 14.35 eV relative to neutral CF_3CH_2F, and therefore 0.16 eV above **TS3**.
[53] K. K. Irikura, W. A. Goddard, and J. L. Beauchamp, "Singlet-triplet gaps in substituted carbenes CXY (X, Y = H, fluoro, chloro, bromo, iodo, silyl)," J. Am. Chem. Soc. **114**(1), 48–51 (1992).
[54] J. Harvey, A. Bodi, R. P. Tuckett, and B. Sztáray, "Dissociation dynamics of fluorinated ethene cations: From time bombs on a molecular level to double-regime dissociators," Phys. Chem. Chem. Phys. **14**(11), 3935 (2012).
[55] J. Harvey, R. P. Tuckett, and A. Bodi, "Shining new light on the multifaceted dissociative photoionisation dynamics of CCl_4," Phys. Chem. Chem. Phys. **16**(38), 20492–20499 (2014).
[56] A. Bodi, P. Hemberger, and R. P. Tuckett, "Coincident velocity map image reconstruction illustrated by the single-photon valence photoionisation of CF_3SF_5," Phys. Chem. Chem. Phys. **19**(44), 30173–30180 (2017).
[57] U. Boesl, "Time-of-flight mass spectrometry: Introduction to the basics," Mass Spectrom. Rev. **36**(1), 86–109 (2017).
[58] R. Lindner, K. Müller-Dethlefs, E. Wedum, K. Haber, and E. R. Grant, "On the shape of $C_6H_6^+$," Science **271**(5256), 1698–1702 (1996).
[59] V. Perebeinos, P. B. Allen, and M. Pederson, "Reexamination of the Jahn-Teller instability in $C_6H_6^+$ and $C_6H_6^-$," Phys. Rev. A **72**(1), 012501 (2005).
[60] K. Krogh-Jespersen, "Ab initio electronic structure calculations on the benzene dication and other $C_6H_6^{2+}$ isomers," J. Am. Chem. Soc. **113**(2), 417–423 (1991).
[61] J. Jašík, D. Gerlich, and J. Roithová, "Probing isomers of the benzene dication in a low-temperature trap," J. Am. Chem. Soc. **136**(8), 2960–2962 (2014).
[62] F. Fantuzzi, D. W. O. de Sousa, and M. A. Chaer Nascimento, "Chemical bonding in the pentagonal-pyramidal benzene dication and analogous isoelectronic hexa-coordinate species," Comput. Theor. Chem. **1116**, 225–233 (2017).
[63] P. Pozo-Guerron, L. E. Seijas, J. L. Burgos, L. Rincon, F. J. Torres, J. R. Mora, C. Zambrano, and R. Almeida, "A topological study of the haxacoordinated carbon in the pentagonal-pyramidal benzene and hexamethylbenzene dications," Chem. Phys. Lett. **758**, 137912 (2020).
[64] W. Wolff, A. Perlin, R. R. Oliveira, F. Fantuzzi, L. H. Coutinho, F. d. A. Ribeiro, and G. Hilgers, "Production of long-lived benzene dications from electron impact in the 20–2000 eV energy range combined with the search for global minimum structures," J. Phys. Chem. A **124**(44), 9261–9271 (2020).
[65] J. Roithová, D. Schröder, P. Gruene, T. Weiske, and H. Schwarz, "Structural aspects of long-lived $C_7H_8^{2+}$ dications generated by the electron ionization of toluene," J. Phys. Chem. A **110**(9), 2970–2978 (2006).
[66] T. Monfredini, F. Fantuzzi, M. A. C. Nascimento, W. Wolff, and H. M. Boechat-Roberty, "Single and double photoionization and photodissociation of toluene by soft X-rays in a circumstellar environment," Astrophys. J. **821**(1), 4 (2016).
[67] U. Jacovella, G. da Silva, and E. J. Bieske, "Unveiling new isomers and rearrangement routes on the $C_7H_8^+$ potential energy surface," J. Phys. Chem. A **123**(4), 823–830 (2019).
[68] J. C. Santos, F. Fantuzzi, H. M. Quitián-Lara, Y. Martins-Franco, K. Menéndez-Delmestre, H. M. Boechat-Roberty, and R. R. Oliveira, "Multiply charged naphthalene and its $C_{10}H_8$ isomers: Bonding, spectroscopy, and implications in AGN environments," Mon. Not. R. Astron. Soc. **512**(4), 4669–4682 (2022).
[69] H. M. Quitián-Lara, F. Fantuzzi, R. R. Oliveira, M. A. C. Nascimento, W. Wolff, and H. M. Boechat-Roberty, "Dissociative single and double photoionization of biphenyl ($C_{12}H_{10}$) by soft X-rays in planetary nebulae," Mon. Not. R. Astron. Soc. **499**(4), 6066–6083 (2020).
[70] A. Y. Pereverzev, C. Rossi, and J. Roithová, "Isomerisation of phenanthrene dication studied by tagging photodissociation ion spectroscopy and DFT calculations," Mol. Phys. **122**, e2225644 (2023).
[71] F. Fantuzzi, L. Baptista, A. B. Rocha, and H. M. Boechat-Roberty, "Positive molecular ions and ion-neutral complexes in the gas phase: Structure and stability of $C_2H_4O_2^{+\cdot}$ and $C_2H_4O_2^{2+}$ isomers," Int. J. Quantum Chem. **112**(20), 3303–3311 (2012).
[72] G. Frenking, W. Koch, and H. Schwarz, "Theoretical investigations on fluorine-substituted ethylene dications $C_2H_nF_{4-n}^{2+}$ (n = 0–4)," J. Comput. Chem. **7**(4), 406–416 (1986).
[73] F. Fantuzzi, B. Rudek, W. Wolff, and M. A. C. Nascimento, "Doubly and triply charged species formed from chlorobenzene reveal unusual C–Cl multiple bonding," J. Am. Chem. Soc. **140**(12), 4288–4292 (2018).
[74] M. C. Bayer, C. Kremser, C. Jessen, A. Nitzer, and A. J. Kornath, "Strengthening of the C–F bond in fumaryl fluoride with superacids," Chem. Eur. J. **28**(15), e202104422 (2022).
[75] A. L. Perlin, W. Wolff, and R. R. Oliveira, "Low energy isomers and infrared spectra simulations of C_4H_3N, C_4H_4N, and C_4H_5N and related ions," J. Phys. Chem. A **127**(11), 2481–2488 (2023).
[76] B. Cordero, V. Gómez, A. E. Platero-Prats, M. Revés, J. Echeverría, E. Cremades, F. Barragán, and S. Alvarez, "Covalent radii revisited," Dalton Trans. **21**, 2832 (2008).